Supplementary Appendix to:

Walking crowds on a shaky surface: Stable walkers discover Millennium bridge oscillations with and without pedestrian synchrony

Varun Joshi and Manoj Srinivasan
Department of Mechanical and Aerospace Engineering
The Ohio State University

S1 Rationale for biped model selection

Independent of the literature on pedestrian-induced bridge oscillations, numerous previous studies have considered the mechanics of bipedal walking and running, some focusing on energetics and some focusing on stability and control [1, 2, 3, 4, 5, 6, 7, 8, 9, 10, 11, 12, 13, 14, 15]. Further mathematical models proposed with the motivation of understanding interactions with a bridge include mathematical abstractions of human locomotion [16, 17], linear inverted pendulums which assume that humans stay nearly vertical [18, 19] and more complicated walkers with springs and dampers that use ad-hoc external forces to maintain stability [20]. The inverted pendulum model used here is just one of many such models, but we feel that it provides a better approximation to actual human motion while remaining computationally tractable.

The inverted pendulum model is certainly (and intentionally) an extreme simplification of the complex dynamics that attend the human body and indeed the human walking motion. It is perhaps the simplest walking model that captures key features of walking stability, specifically the instability due to inverted pendulum-like body dynamics and stabilization using foot placement. Further, as noted in the main manuscript, our weighting of absolute and relative sideways velocity error in the foot placement controller promotes stability despite surface motions and models humans weighting different sensors to produce a coherent state estimate [21]. In addition to simplifying the human body to having a point-mass upper body and massless legs with no swing dynamics, the walking motion itself is simplified in a manner that there is no double stance phase and there is no change in direction. Our simulated walkers have a preferred straight line walking direction, whereas in a real crowd, walkers may occasionally change direction to avoid another pedestrian, a feature we hope to incorporate in future work.

Previous models used to simulate interactions of bipeds with a bridge were 2D models restricted to the frontal plane and they did not have the ability to walk forward or the ability to fall to the ground (a key aspect of walking stability). It is known that fore-aft and sideways walking dynamics are indeed coupled [8]. A biped that is stabilized in the sideways direction may still fall forward, so it may not be accurate to ignore the forward walking dynamics.

S2 Body equations of motion

For the model shown in figure 1 of main manuscript, there are two forces acting on the center of mass during single stance, namely, the force along the leg F and the weight of the biped mg, where m is the biped mass, and g is acceleration due to gravity. The lateral, forward and vertical positions of the body center of mass (CoM) are given by x, y and z respectively and the stance foot position in contact with the ground is given by $(x_{\text{foot}}, y_{\text{foot}}, z_{\text{foot}})$. The leg length is ℓ, given by,

$$\ell^2 = (x - x_{\text{foot}})^2 + (y - y_{\text{foot}})^2 + (z - z_{\text{foot}})^2 \,. \tag{1}$$

where $z_{\text{foot}} = 0$. The equations of motion for the center of mass are:

$$m\ddot{x} = F\,\frac{x - x_{\text{foot}}}{\ell}, \tag{2}$$

$$m\ddot{y} = F\,\frac{y - y_{\text{foot}}}{\ell}, \text{ and} \tag{3}$$

$$m\ddot{z} = F\,\frac{z - z_{\text{foot}}}{\ell} - mg, \tag{4}$$

which are applicable for all versions of the biped model. Recall that non-dimensionalization is performed by dividing by appropriate combinations of mass m, inverted pendulum leg length ℓ_0, and acceleration due to gravity g. In the following, we denote the non-dimensional analogues of dimensional quantities by adding an overbar; for instance, fore-aft position $\bar{y} = y/\ell_0$, non-dimensional leg force $\bar{F} = F/(mg)$, non-dimensional speed $\bar{v} = v/\sqrt{g\ell_0}$, and non-dimensional time $\bar{t} = t\sqrt{g/\ell_0}$. The origin for all position measurements is the current stance-foot position.

S3 Platform equations of motion

To simulate the bridge, we add another equation for the motion $X(t)$ of the bridge in the lateral direction:

$$M\ddot{x}_{\text{platform}} + B\dot{x}_{\text{platform}} + Kx_{\text{platform}} = -F \cdot \frac{x - x_{\text{foot}}}{\ell} \tag{5}$$

where K and B are the stiffness and damping of the platform in the lateral direction respectively, and M is the appropriate modal mass of the bridge.

To simulate an externall shaken treadmill, the platform motion is specified as sinusoidal, of the form:

$$x_{\text{platform}} = A_{\text{platform}} \sin\left(\omega_{\text{platform}} t + \phi\right) \tag{6}$$

where A_{platform} is the amplitude, ω_{platform} is the frequency of oscillation, and ϕ is the phase difference between the biped stride and the platform oscillation.

S4 Leg force equations

The biped is assumed to perform an exact 3D inverted pendulum motion, we use a differential algebraic equation formulation to enforce the leg length constraint. We do not fix the leg length, but rather constrain the motion of the center of mass to be such that the leg length cannot change from the

beginning of the motion. The second derivative of this leg length constraint (equation 1) produces the following additional ODE:

$$(x - x_{\text{foot}})\,\ddot{x} + (y - y_{\text{foot}})\,\ddot{y} + (z - z_{\text{foot}})\,\ddot{z} = -\left(\dot{x} - \dot{x}_{\text{platform}}\right)^2 - \dot{y}^2 - \dot{z}^2 + \ddot{x}_{\text{platform}}\,(x - x_{\text{foot}}) \tag{7}$$

This equation, along with the equations 2-4 can be combined to determine the acceleration of the center of mass and the force along the leg. For the finite inertia platform, we add equation 5 to these equations to get the lateral acceleration of the platform as well.

S5 Impulse equations

At the end of each biped stance phase a push-off impulse is applied to coupled system along the leg of the biped. These impulses directly affect the momentum of the biped CoM and the platform.

$$m\dot{x}_{\text{post-push-off}} = m\dot{x}_{\text{pre-push-off}} + I_{\text{push-off}} \cdot \frac{x - x_{\text{foot}}}{\ell_0}, \tag{8}$$

$$m\dot{y}_{\text{post-push-off}} = m\dot{y}_{\text{pre-push-off}} + I_{\text{push-off}} \cdot \frac{y - y_{\text{foot}}}{\ell_0} \tag{9}$$

$$m\dot{z}_{\text{post-push-off}} = m\dot{z}_{\text{pre-push-off}} + I_{\text{push-off}} \cdot \frac{z - z_{\text{foot}}}{\ell_0}, \tag{10}$$

In the finite inertia case, we also use equation 11.

$$m_{\text{platform}}\dot{x}_{\text{platform,post-push-off}} = m_{\text{platform}}\dot{x}_{\text{platform,pre-push-off}} + I_{\text{push-off}} \cdot \frac{x_{\text{foot}} - x}{\ell_0} \tag{11}$$

After the push-off, we solve for the value of the heel-strike impulses for each biped that would make the leg-length-rate of the biped 0, thus insuring continued inverted pendular motion, we apply the heel-strike impulse similar to equations 8 - 10.

S6 Order parameter equations

In order to compute the order parameter we first define the phase of a biped. We use step-length and CoM position to determine phase:

$$\phi = 2\pi \frac{y}{y_{\text{foot}}} \tag{12}$$

Where both y and y_{foot} are measured with the stance-foot as the origin. The magnitude of the order parameter is computed as follows [22]:

$$r = \left| \frac{1}{P} \sum_{j=1}^{P} e^{i\phi_j} \right| \tag{13}$$

where ϕ_j is the phase of the j^{th} biped and P is the total number of simulated bipeds.

S7 Simulation parameters

We use $\bar{k}_1 = 1$, $\bar{k}_2 = 2$, $\bar{k}_3 = 2$ and $\bar{k}_4 = -0.5$ for the non-dimensional control gains in our foot-placement and push-off feedback controllers. The non-dimensional biped speed is set to be 0.3.

For the finite inertia platform, the nominal values of mass, stiffness, and damping are identical to those used in [16] as approximating the London Millennium Bridge: $M = 1.13 \times 10^5$ kg, $B = 1.1 \times 10^4$ Nsm^{-1}, and $K = 4.73 \times 10^6$ Nm^{-1}.

For non-dimensionalization, we used human mass $m = 70$ kg, maximum leg length $\ell_0 = 1$ m, and $g = 9.81$ ms^{-1}. Small changes to these values do not affect the qualitative results presented in this article.

S8 Metabolic cost model

The metabolic cost function contains the following four terms, identical to those defined by Joshi and Srinivasan [4]:

1. the resting metabolic rate, the metabolic rate while not moving, about 1.4 Watts per kg [23]. The cost of locomotion is, as below, over and above this resting cost.
2. the stance work cost, a work-based metabolic cost term, a linear combination of the positive and negative work performed by the leg. We use an average positive work efficiency of 25% ($\eta_{\mathrm{pos}} = 0.25$) and negative work efficiency of 120% ($\eta_{\mathrm{neg}} = 1.2$) [1, 2]. The work is done by the biped only during the push-off and heel-strike impulses.
3. the swing leg cost is the the cost of moving the swing leg from stance phase to the next, again quantifies by a linear combination of the positive and negative work as before.
4. and the stance force cost, the integral of the force along the leg.

The sum of these four cost terms, per unit distance, is non-dimensionalized to estimate of the 'cost of transport' of walking [24, 25].

S9 Mathematical remarks on entrainment

Resonance. The classic notion of a resonance is a phenomenon in linear dynamical systems, in which a structure (such as a bridge) with a particular natural frequency of passive vibration f_n is excited by some external periodic force with frequency close to f_n. In such cases, the applied external force is not generally affected by the motion of the system. The phenomena considered here cannot fully be understood using ideas and intuition drawn from resonance. First, in our bridge-pedestrian case, the pedestrians and the bridge, and there is two-way coupling between the two. The pedestrians are affected by the bridge and vice versa. Further, If the pedestrians walk with zero step width initially, which was our assumption for simplicity, there is no initial sideways forcing on the bridge. So it is

the instability of this planar periodic motion that gives rise to the steady state bridge motion. Such instability-driven forcing of structures and having multiple regimes of oscillation versus no oscillation are not part of the phenomenology of resonance.

Phase response curves. The formal mathematics of entrainment and synchrony usually invoke the notion of 'phase response curves', which characterize how an asymptotically stable oscillator such as a human walker is affected by a discrete external perturbation such as the sudden and brief movement of the ground or a discrete pull from the outside [26, 22]. Then, a continuous or periodic external forcing such as due to a bridge can be considered as a sum over such brief forces, and the resulting response of the bipedal walker by integrating over the forcing function (by 'convolving' the forcing and the phase response curve). The technically correct use of the phase response curves requires that the bridge and the pedestrians are weakly coupled. Such weak coupling assumption is a good approximation when a few pedestrians are coupled to the massive bridge, shaking slightly, so that the bridge can affect the person, but the person cannot affect the bridge; the same is true for the response to a slightly shaken treadmill. However, once we have hundreds of pedestrians on the bridge or if the bridge or treadmill moves substantially, the weak coupling assumption may not be accurate. The use of phase response curves for the mathematical analysis of human-bridge coupling is beyond the scope of this article.

Limiting cases. As alluded to in the previous paragraph, independent of the use of the phase response curves, it may be insightful to consider some limiting cases of the coupled pedestrian-human system. Given that the entrainment occurs only when the pedestrian mass becomes large enough, it may be useful to consider the limit of infinitesimal bridge mass. But the limit of truly zero bridge mass with non-zero stiffness and zero damping leads to a mathematically singular limit that does not allow inverted pendular walking. This is because the push-off and heel-strike impulses from the human will create infinite sideways bridge speeds due to the zero bridge mass and damping. It may be possible to consider a bridge with zero mass, but with non-zero damping and stiffness, but this limit is not much more analytically tractable and also requires some simulation.

S10 An impulsively stabilized inverted pendulum

We have used a mechanistically-motivated feedback controller for human walking to show that bridge-shaking naturally emerges from these dynamics coupled to the bridge. We hypothesize that the primary dynamical mechanism needed for the bridge to shake sideways is some 'feedback controller' that corrects a sideways fall by applying a restoring sideways force against the substrate roughly periodically. We now provide a second example supporting this hypothesis.

Consider an inverted pendulum 'standing' on a platform (such as a bridge), attached to the world through a spring (figure S7a). The inverted pendulum is stabilized by an ankle torque impulse, applied once every T time units. The stabilizing ankle torque impulse P_{ankle} uses a proportional-derivative controller, proportional to the inverted pendulum angle and angular velocity: $P_{\text{ankle}} = -k_p\theta - k_d\dot{\theta}$. The linearized coupled equations of motion for the bridge and the inverted pendulum are of the form:

$$M\ddot{x}_{\text{platform}} + Kx_{\text{platform}} + C\dot{x}_{\text{platform}} = F, \quad \text{and } m\ddot{x} + F = 0$$

where m is the mass of the point-mass in the inverted pendulum, F is the horizontal interaction force between the pendular mass and the bridge due to passive pendular dynamicss, and angle $\theta =$

$(x - x_{\text{platform}})/\ell$. To simulate the effect of multiple synchronized inverted pendula, we can scale the mass m, the interaction force F, and the gains k_p and k_d by the number of pendula N. For low N, the vertical position of the inverted pendulum is stable ($\theta = 0$) due to the feedback controller, but for large N, the vertical position becomes unstable giving rise to platform oscillations (figure S7b), quite similar to those observed in the walking simulations described in the main manuscript.

A related problem is related to the art of slack-lining, in which a person walks on a thin elastic band tied between two poles [27], in which one observes uncontrolled oscillations of the feet and the elastic band when the feedback control has a delay between sensing and actuation, rather like the implicit delay between successive actions during walking or the impulsively stabilized walker described above. Similarly, continuous (non-impulsive) stabilization of inverted pendulum using a traditional PD controller goes unstable at large delay in the feedback [28].

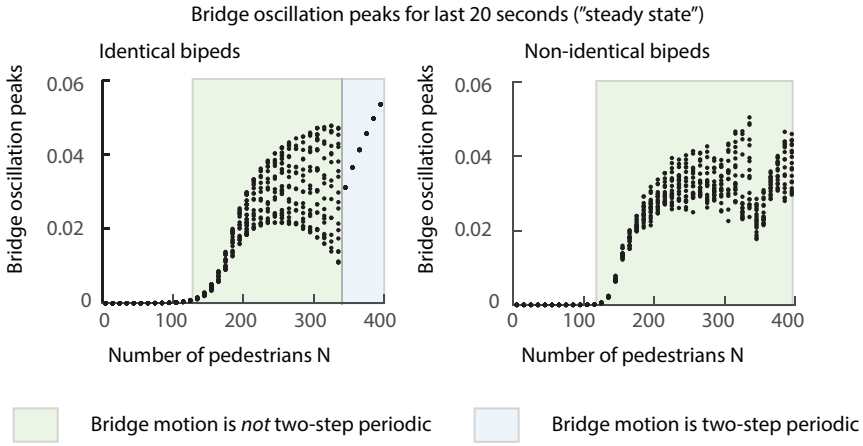

Figure S1: **An "orbit diagram" illustrating complex motions of the bridge and dependence of bridge "amplitude" on N.** At each pedestrian number N, we perform a long simulation. From this long simulation, we obtained the 'peaks' of the bridge oscillations (i.e. the maximum rightward bridge deviations from its static position) from the last 20 seconds of the simulation. We plot all of these oscillation peaks as a function of N. If all oscillation peaks are identical, we obtain a single point per N, as in the $N > 350$ regime for identical bipeds – corresponding to the bridge having the same period as two human steps. If the oscillation peaks are different, as in a multi-step periodic motion or a non-periodic motion, the points represent the various oscillation peaks that the bridge goes through.

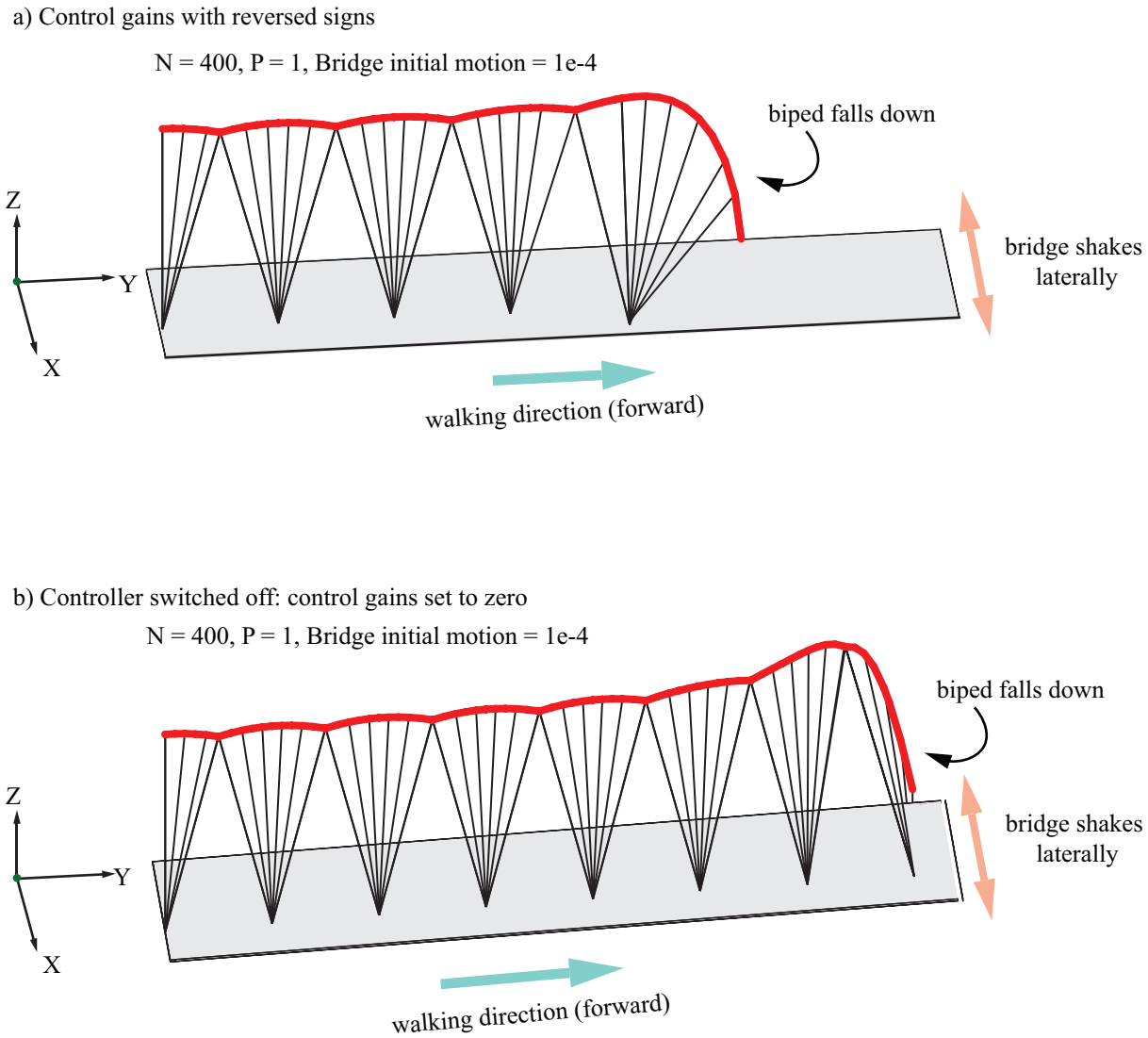

Figure S2: **Bad controllers make the biped fall.** Biped body trajectory is shown for two different "bad" feedback controllers, and both these controllers results in the biped falling in a few steps. a) Controller with all feedback gains in the model are reversed in sign. b) Controller with all feedback gains set to zero. Both simulations start with the same small initial bridge oscillation. We notice that the biped with the zero gain controller falls later than the biped with the reversed-sign-gains controller.

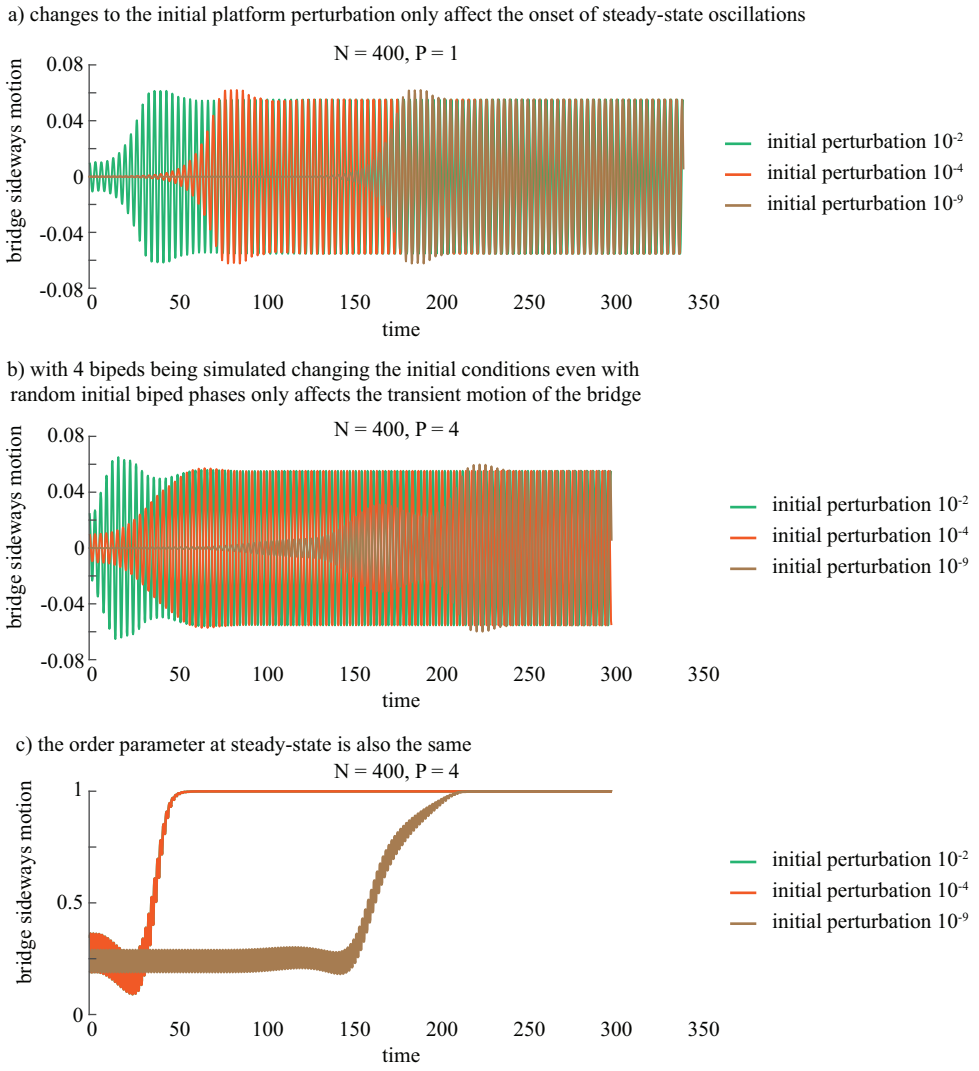

Figure S3: **Steady state is independent of bridge and pedestrian initial conditions.** a) The steady state bridge oscillations do not depend on initial conditions, but smaller initial bridge deviation implies a longer time duration to reach near steady-state. b) The bridge's steady state does not depend on the initial conditions of pedestrians, whereas the transients do depend on the initial conditions. c) The $P = 4$ bipeds simulated synchronize despite random pedestrial initial conditions and different initial bridge deviations.

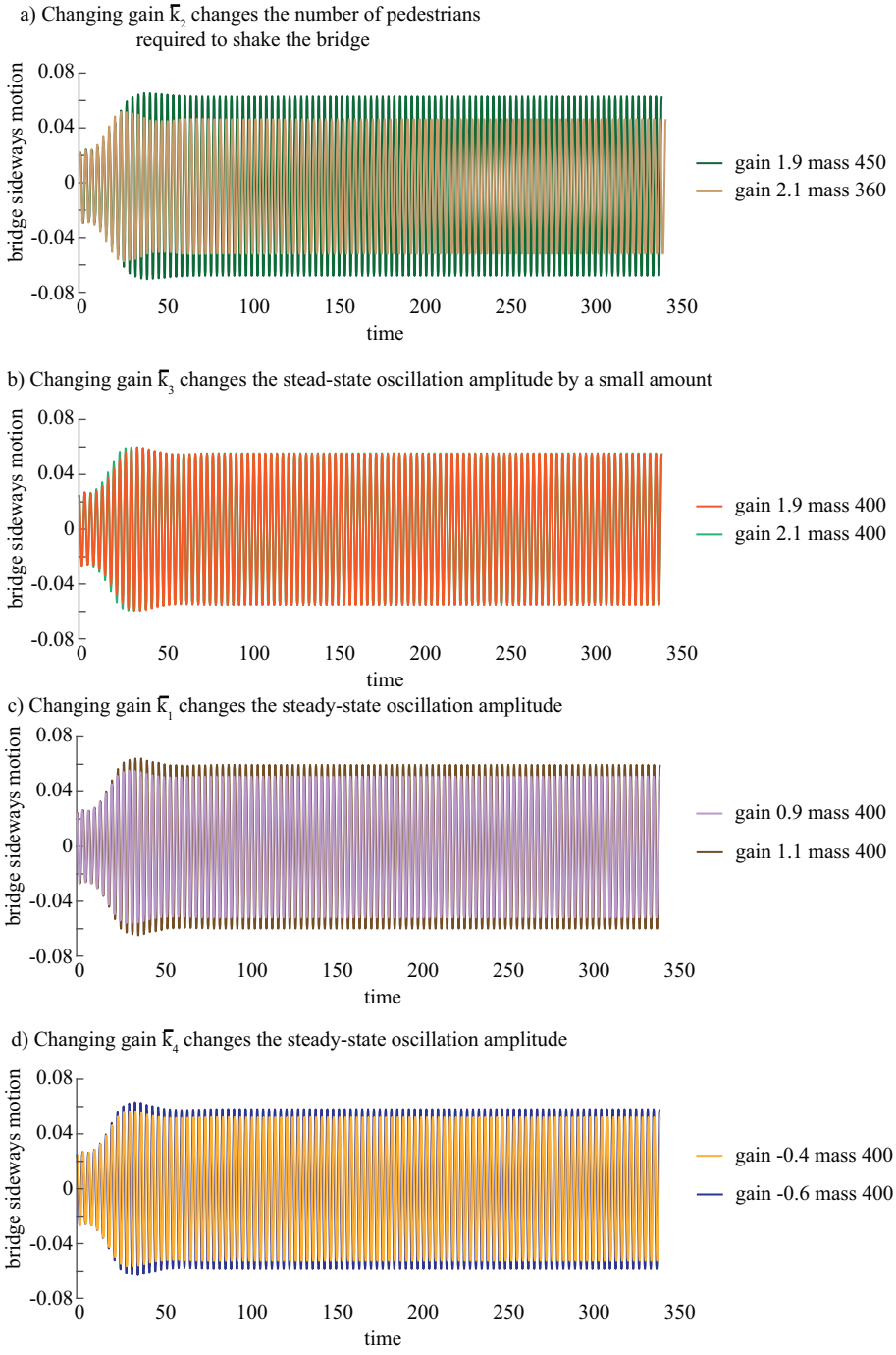

Figure S4: **Bridge-shaking behavior is seen for a range of feedback gain values.** Steady state bridge oscillations are shown for a range of feedback gain parameters, suggesting some robustness of the observed behavior to chosen gain values. However, as noted in Figure S2, this robustness does not extend to large changes in gains, such as reversing their signs or setting them equal to zero.

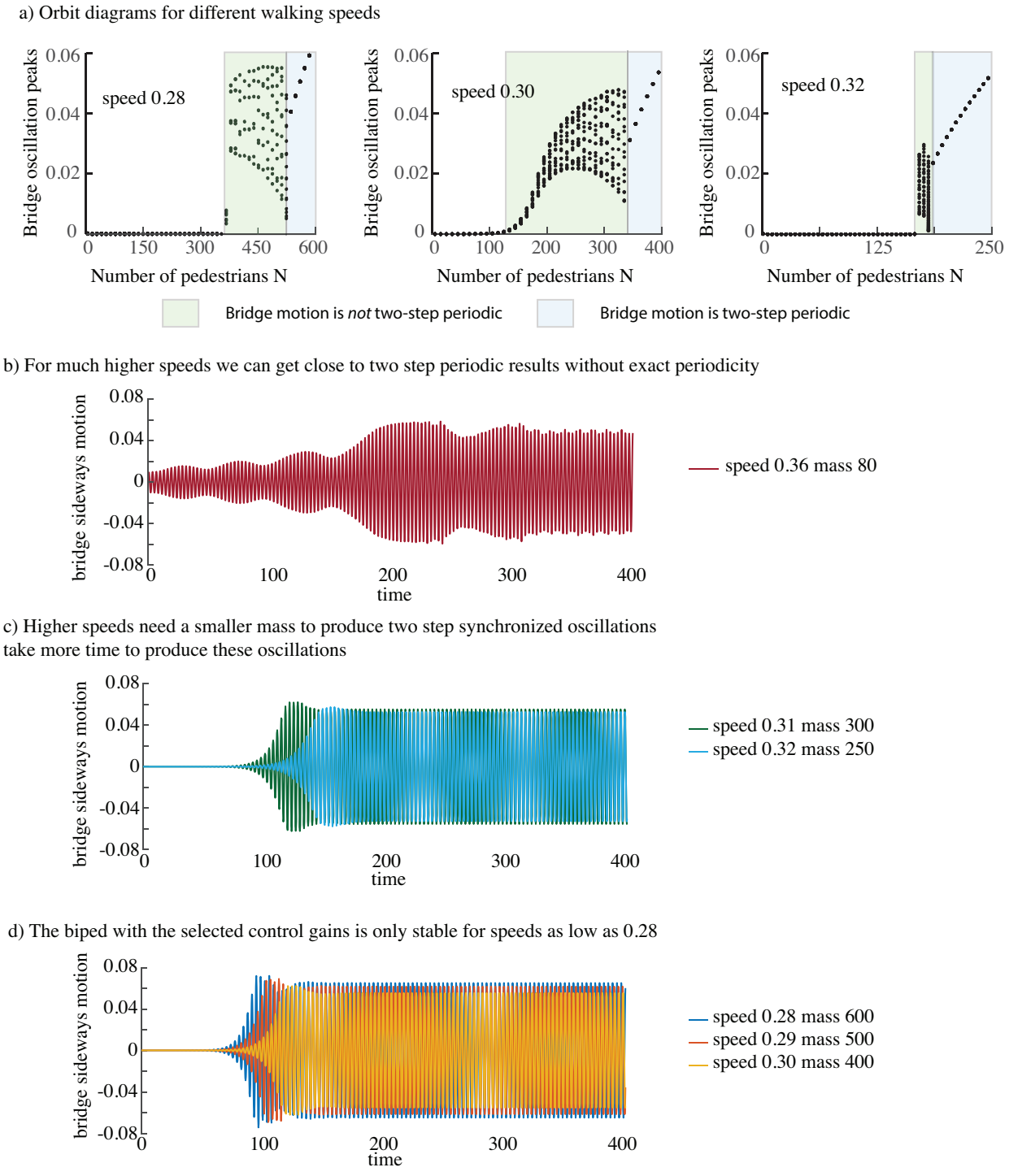

Figure S5: **Bridge-shaking behavior is seen for a range of speeds.** a) The bridge amplitude as a function of effective pedestrian number is shown as an orbit diagram for three different speeds. The same three qualitative regimes are seen for the different speeds, albeit with different ranges for each regime. b, c, d) Bridge motion is shown for different speeds and correspondingly numbers of pedestrians to qualitatively illustrate that the bridge-shaking behavior is seen for a range of speeds. For larger speeds, for given controller gains, the bridge settles into a periodic motion for a smaller number of pedestrians.

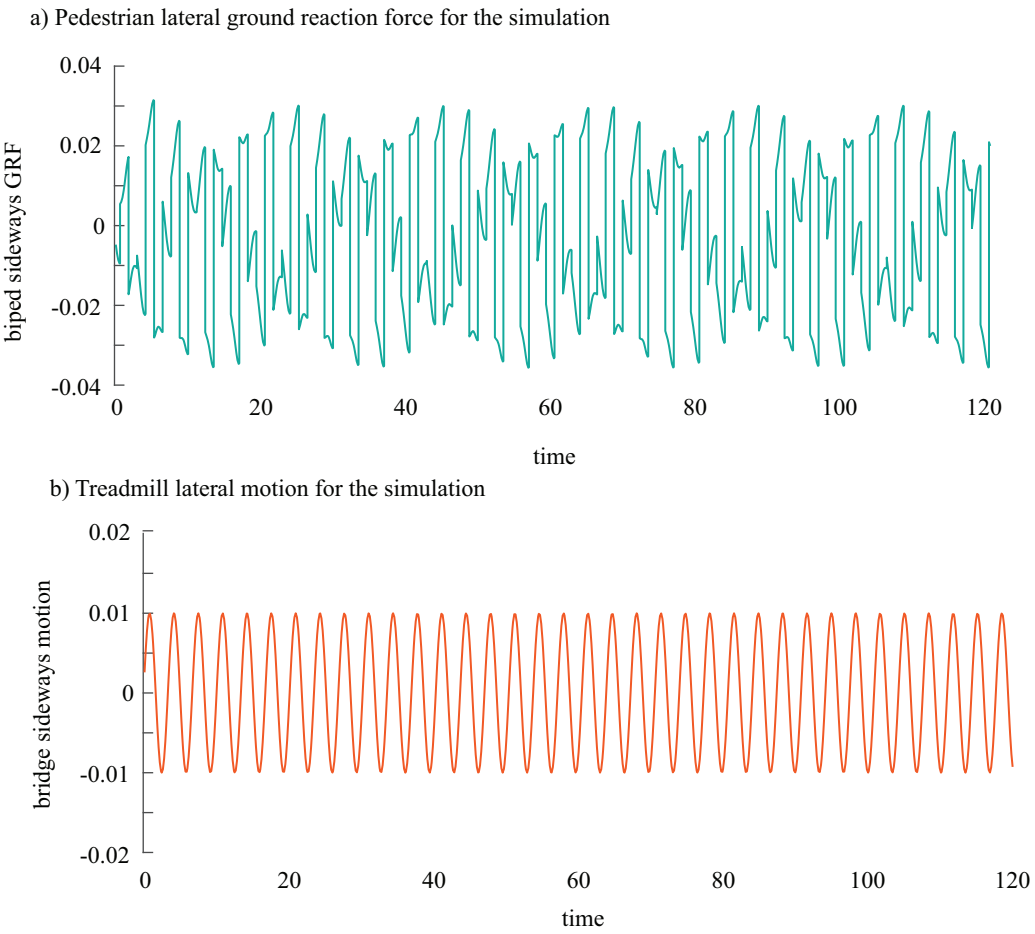

Figure S6: **Lateral reaction forces on a shaken platform.** The plots are from simulations of a single biped walking on a treadmill that shakes sinusoidally with the following parameters: pedestrian forward walking speed = 0.5 (non-dimensional) = 1.56 m/s platform lateral shaking amplitude = 0.01 (non-dimensional) = 1 cm, and platform lateral shaking frequency = 0.3 (non-dimensional) = 0.94 Hz. The ground reaction forces have two dominant frequencies, resulting in a 'beating' oscillation as in [29]. For other parameters, when the person entrains to the platform one-to-one, the lateral reaction forces are simply periodic at the shaking frequency, without the beating character.

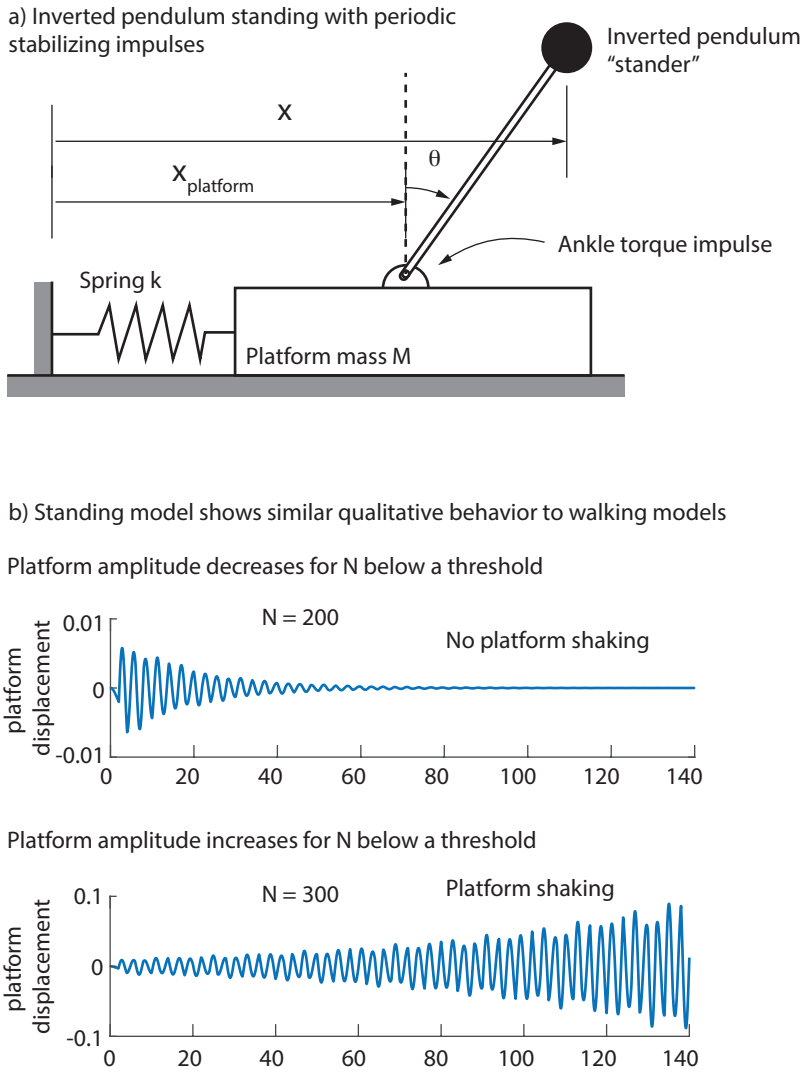

Figure S7: **Impulsive inverted pendulum standing.** a) An inverted pendulum pivots about its "ankle" on a platform. For consistency, the platform has the same properties as the Millennium Bridge and the inverted pendulum has the same mass and length as the biped models discussed earlier. The impulsive torques are applied at the frequency of normal human walking. b) When we scale the pendulum properties (mass, feedback gains, and interaction forces) by the number of bipeds N, we obtain decaying platform oscillations for low N (e.g., $N = 200$) and growing platform oscillations for larger N (e.g., $N = 300$).

References

[1] A. D. Kuo, J. M. Donelan, and A. Ruina, "Energetic consequences of walking like an inverted pendulum: step-to-step transitions.," *Exercise and sport sciences reviews*, vol. 33, pp. 88–97, Apr. 2005.

[2] M. Srinivasan, "Fifteen observations on the structure of energy minimizing gaits in many simple biped models," *J R Soc Interface*, vol. 8, pp. 74–98, 2011.

[3] M. Srinivasan and A. Ruina, "Computer optimization of a minimal biped model discovers walking and running," *Nature*, vol. 439, no. 7072, p. 72, 2006.

[4] V. Joshi and M. Srinivasan, "Walking on a moving surface: energy-optimal walking motions on a shaky bridge and a shaking treadmill can reduce energy costs below normal," *Proc R Soc A*, vol. 471, p. 20140662, 2015.

[5] S. Song and H. Geyer, "Generalization of a muscle-reflex control model to 3D walking," *P Ann Int IEEE EMBS*, no. Eec 0540865, pp. 7463–7466, 2013.

[6] A. Seyfarth, H. Geyer, and H. Herr, "Swing-leg retraction: a simple control model for stable running," *Journal of Experimental Biology*, vol. 206, no. 15, pp. 2547–2555, 2003.

[7] S. Kuindersma, F. Permenter, and R. Tedrake, "An efficiently solvable quadratic program for stabilizing dynamic locomotion," in *Robotics and Automation (ICRA), 2014 IEEE International Conference on*, pp. 2589–2594, IEEE, 2014.

[8] Y. Wang and M. Srinivasan, "Stepping in the direction of the fall: the next foot placement can be predicted from current upper body state in steady-state walking.," *Biol lett*, vol. 10, pp. 1–9, 2014.

[9] C. E. Bauby and A. D. Kuo, "Active control of lateral balance in human walking," *Journal of biomechanics*, vol. 33, no. 11, pp. 1433–1440, 2000.

[10] M. Kim and S. H. Collins, "Once-per-step control of ankle push-off work improves balance in a three-dimensional simulation of bipedal walking," *IEEE Trans Robot*, pp. 1–13, 2017.

[11] H. Geyer, A. Seyfarth, and R. Blickhan, "Compliant leg behaviour explains basic dynamics of walking and running," *Proceedings of the Royal Society of London B: Biological Sciences*, vol. 273, no. 1603, pp. 2861–2867, 2006.

[12] M. A. Daley and J. R. Usherwood, "Two explanations for the compliant running paradox: reduced work of bouncing viscera and increased stability in uneven terrain," *Biology Letters*, vol. 6, no. 3, pp. 418–421, 2010.

[13] R. H. Miller, "A comparison of muscle energy models for simulating human walking in three dimensions," *Journal of biomechanics*, vol. 47, no. 6, pp. 1373–1381, 2014.

[14] F. C. Anderson and M. G. Pandy, "Dynamic optimization of human walking," *Journal of biomechanical engineering*, vol. 123, no. 5, pp. 381–390, 2001.

[15] M. Ackermann and A. J. Van den Bogert, "Optimality principles for model-based prediction of human gait," *Journal of biomechanics*, vol. 43, no. 6, pp. 1055–1060, 2010.

[16] S. H. Strogatz, D. M. Abrams, A. McRobie, B. Eckhardt, and E. Ott, "Theoretical mechanics: crowd synchrony on the Millennium Bridge.," *Nature*, vol. 438, pp. 43–4, 2005.

[17] I. Belykh, R. Jeter, and V. Belykh, "Foot force models of crowd dynamics on a wobbly bridge," *Science advances*, vol. 3, no. 11, p. e1701512, 2017.

[18] J. Macdonald, "Lateral excitation of bridges by balancing pedestrians," *Proc R Soc A*, pp. 1055–1073, 2008.

[19] M. Bocian, J. H. Macdonald, and J. F. Burn, "Biomechanically inspired modeling of pedestrian-induced vertical self-excited forces," *Journal of Bridge Engineering*, vol. 18, no. 12, pp. 1336–1346, 2013.

[20] Q. Yang, J. Qin, and S. Law, "A three-dimensional human walking model," *Journal of Sound and Vibration*, vol. 357, pp. 437–456, 2015.

[21] S. Hwang, P. Agada, T. Kiemel, and J. J. Jeka, "Dynamic reweighting of three modalities for sensor fusion," *PLoS ONE*, vol. 9, p. e88132, 2014.

[22] S. H. Strogatz, "From Kuramoto to Crawford: exploring the onset of synchronization in populations of coupled oscillators," *Physica D*, vol. 143, pp. 1–20, 2000.

[23] A. Bobbert, "Energy expenditure in level and grade walking," *Journal of Applied Physiology*, vol. 15, no. 6, pp. 1015–1021, 1960.

[24] V. A. Tucker, "Energetic cost of locomotion in animals," *Comparative Biochemistry and Physiology*, vol. 34, no. 4, pp. 841–846, 1970.

[25] S. Collins, A. Ruina, R. Tedrake, and M. Wisse, "Efficient bipedal robots based on passive-dynamic walkers," *Science*, vol. 307, no. 5712, pp. 1082–1085, 2005.

[26] B. Clark, *Energy economy and stability in bipedal locomotion with energy-optimal perturbation rejection*. PhD thesis, the Ohio State University, 2018.

[27] P. Paoletti and L. Mahadevan, "Balancing on tightropes and slacklines," *Journal of The Royal Society Interface*, vol. 9, no. 74, pp. 2097–2108, 2012.

[28] J. Milton, J. L. Cabrera, T. Ohira, S. Tajima, Y. Tonosaki, C. W. Eurich, and S. A. Campbell, "The time-delayed inverted pendulum: implications for human balance control," *Chaos: An Interdisciplinary Journal of Nonlinear Science*, vol. 19, no. 2, p. 026110, 2009.

[29] D. Claff, M. Williams, and A. Blakeborough, "The kinematics and kinetics of pedestrians on a laterally swaying footbridge," *Journal of Sound and Vibration*, vol. 407, pp. 286–308, 2017.

[30] M. Bocian, J. Macdonald, and J. Burn, "Biomechanically inspired modelling of pedestrian-induced forces on laterally oscillating structures," *J Sound Vib*, vol. 331, pp. 3914–3929, 2012.

Paper	**Pedestrian Model**	**Controller**	**3D**	**Bridge Model**	**Multiple Pedestrians**	**Pedestrian response to bridge motion**
Belykh 2017 [17]	Phase oscillator	Phase coupling with bridge	No	Phase oscillator which responds to pedestrian motion	Yes and pedestrians can have different parameters	Phase can change as a function of bridge motion
Strogatz 2005 [16]	Phase oscillator	Phase coupling with bridge	No	Phase oscillator which responds to pedestrian motion	Yes	Phase can change as a function of bridge motion
Bocian 2013[19]	Inverted pendulum	Impulse maintains linear momentum	No	Vertically shaking bridge with sinusoidal motion	No	Step-timing can change in response to bridge motion
Bocian 2012 [30]	Linear inverted pendulum	Hof foot placement model	No	Multiple bridge vibration modes driven by pedestrian motion	Yes	Lateral foot-position can change in response to bridge motion
Joshi Srinivasan 2014 [4]	Point-mass with telescoping legs	Energy minimizing feed-forward optimal trajectory	Yes	Lateral spring-mass-damper model	No	Just periodic motion
Joshi Srinivasan 2018	Inverted Pendulum	Linear controller based on human foot-placement with an ad-hoc linear push-off impulse law	Yes	Lateral spring-mass-damper bridge	Yes and pedestrians can have different parameters	Step-length, step-width and push-off impulse can change in response to bridge motion

Table S1: Features of some previous articles on 3D walking or interaction with bridge surface, showing how our article is distinct from them.